SCIENCE CHINA
Technological Sciences

•Article•

January 2023 Vol.66 No.1: 173–180
https://doi.org/10.1007/s11431-022-2237-5

Tailoring the mechanical properties of bulk metallic glasses via cooling from the supercooled liquid region

ZHANG LangTing[1], DUAN YaJuan[1,2], WANG YunJiang[3,4], YANG Yong[5,6] & QIAO JiChao[1,7*]

[1] *School of Mechanics, Civil Engineering and Architecture, Northwestern Polytechnical University, Xi'an 710072, China;*
[2] *Department of Physics, Barcelona Research Center in Multiscale Science and Technology, Institute of Energy Technologies, Universitat Politècnica de Catalunya, Barcelona 08019, Spain;*
[3] *State Key Laboratory of Nonlinear Mechanics, Institute of Mechanics, Chinese Academy of Sciences, Beijing 100190, China;*
[4] *School of Engineering Science, University of Chinese Academy of Sciences, Beijing 100049, China;*
[5] *Department of Mechanical Engineering, College of Engineering, City University of Hong Kong, Hong Kong 999077, China;*
[6] *Department of Materials Science and Engineering, College of Engineering, City University of Hong Kong, Hong Kong 999077, China;*
[7] *Innovation Center, NPU-Chongqing, Chongqing 401135, China*

Received August 11, 2022; accepted October 19, 2022; published online December 26, 2022

Structural rejuvenation is vital and attractive for modulating the energetic state and structural heterogeneity of bulk metallic glasses (BMGs). In this paper, we show that cooling a BMG from a supercooled liquid region at laboratory rates can reverse the relaxation enthalpy lost during the preceding structural relaxation. Increasing the cooling rate is beneficial for enhancing atomic mobility and dynamic mechanical relaxation intensity. Therefore, this rejuvenation methodology promotes tailoring the mechanical properties of BMGs and provides a comprehensive understanding of the rejuvenation mechanism.

bulk metallic glass, thermal rejuvenation, supercooled liquid region, mechanical relaxation, structural heterogeneity

Citation: Zhang L T, Duan Y J, Wang Y J, et al. Tailoring the mechanical properties of bulk metallic glasses via cooling from the supercooled liquid region. Sci China Tech Sci, 2023, 66: 173–180, https://doi.org/10.1007/s11431-022-2237-5

1 Introduction

Bulk metallic glasses (BMGs), one of the advanced disordered alloys, are actually prepared by rapidly cooling melting liquids [1–5]. Due to their impressive properties, such as ultrahigh strength, high elastic limit, and superior hardness, BMGs have received the interest of materials science and technical science. However, the inevitable structural relaxation induced by physical aging drives BMGs into a stable state; then destroys some inherent properties, such as room plasticity, and seriously restricts their engineering applications [6–8]. In the past decades, structural rejuvenation has been popularly studied, and several strategies have been developed, such as cold-rolling, high-temperature creep, and shock compression [9–15]. These mechanical strategies introduce severe plastic deformation and inevitable mechanical damage to the glassy structure, which causes barriers to clarifying the rejuvenation mechanism of BMGs. Unlike mechanical strategies, thermal methods are more promising for achieving rejuvenation without any mechanical damage. The cyclic cryogenic process has been recently proposed to rejuvenate BMGs, providing an increase in the relaxation enthalpy and an improvement of plasticity [10]. Importantly, rejuvenation in some tellurite glasses was attained upon cooling from the supercooled liquid region (SLR) with laboratory cooling rates. This thermal method is homogenous and applicable, inspiring us to clearly identify the rejuvenation mechanism of BMGs.

* Corresponding author (email: qjczy@nwpu.edu.cn)

The temperature-dependent energetic state of BMGs is the pivotal index for modulating the mechanical properties of glasses and plays an important part in diverse rejuvenation processes. The correlation between mechanical relaxation process, rejuvenation processes, and microstructural heterogeneity have been positively explored in terms of experimental analysis and atomic-scale computer simulations [16–19]. For example, the boson peak gets enhanced and shifts to low-temperature regions with a strong rejuvenation [12]. Meanwhile, the vitalization of the γ relaxation process of BMGs introduces a considerable enthalpy recovery and has been proven as a universal behavior of glasses [20]. The above significant results on the rejuvenation behavior of BMGs are appealing for the study on the link between the rejuvenation mechanism and dynamic mechanical relaxation. However, the effect of the rejuvenation behavior on dynamic mechanical relaxation processes and control of the structural heterogeneity of a rejuvenated BMG are still unknown. These factors will be clarified by the interpretation of the inherent correlation between the rejuvenation behavior achieved by cooling from the SLR and the improvement of dynamic mechanical relaxation.

In the current research, the relationship between structural heterogeneity and structural rejuvenation is established from the dynamic aspect by the heat flow and viscoelastic measurements. The results show that cooling a BMG from the SLR at only a few Kelvins per minute can rejuvenate BMGs and then improve their atomic mobility, which provides a further understanding of rejuvenation and is an effective method to improve their mechanical properties.

2 Experimental procedure

A typical La-based BMG was selected as the model alloy (nominal composition $La_{30}Ce_{30}Ni_{10}Al_{20}Co_{10}$), and as-cast plates with dimensions of approximately 70 mm×10 mm×2 mm were prepared by the copper mold suction casting technique [21].

The amorphous structure of the samples was confirmed via X-ray diffraction (D8, Bruker AXS Gmbh) using Cu Kα radiation. The thermal properties were determined using a differential scanning calorimeter (DSC, NETZSCH DSC 449C) with a heating rate of 20 K/min.

The mechanical spectra were studied on a TA Q850 dynamic mechanical analysis (DMA) in the single-cantilever bending mode. DMA samples with dimensions of approximately 25 mm×2 mm×1 mm were cut by a diamond cutting machine. The complex modulus of the viscoelastic materials in the complex plane is expressed as $E^*=\sigma/\varepsilon=E'+iE''$. E' is the storage modulus correlated to the energy storage part during the deformation, and E'' is the loss modulus correlated to the energy loss part. Applying the periodic stress $\sigma=\sigma_0\cos(2\pi ft)$, the strain response of viscoelastic materials is recorded as $\varepsilon=\varepsilon_0\cos(2\pi ft+\delta)$, where f is the driving frequency and δ is the phase angle. The loss factor $\tan\delta=E''/E'$, a parameter relating to the atomic mobility of BMGs, is also computed.

3 Results and discussion

Figure 1(a) shows the DSC results of $La_{30}Ce_{30}Ni_{10}Al_{20}Co_{10}$ BMG in the initial structure termed Run1 and in the crystalline state (the sample was cooled to 323 K after full crystallization) labeled as Run2. Run1 exhibits an exothermal peak because of the structural relaxation (the glass transition temperature T_g is signed), endothermal peak in the SLR, and strong exothermal heat flow induced by crystallization. No peculiarities were exhibited in the DSC curve of the crystalline alloy (Run2). The quantity $W_{ini}=W_{Run1}-W_{Run2}$ was calculated to obtain the heat flow for BMGs without any contribution of the crystalline counterparts. DSC traces with various proceeding thermal protocols are displayed in the inset of Figure 1(b). After heating into the SLR, the samples were cooled to 323 K at a cooling rate of 1 K/min$\leqslant T_{cooling}\leqslant$20 K/min. After these thermal protocols, the corresponding DSC curves were obtained based on the same method, "Run1−Run2," as shown in Figure 1(b). Taking the cooling rate of 1 K/min as an instance, one can observe that (1) the exothermal peak totally disappears, (2) the intensity of the endothermal peak enhances, and (3) the approximate overlap with an as-cast curve at approximately 500 K. Structural relaxation is characterized by a decrease in the relaxation enthalpy. The heat flow curves apparently shift toward the as-cast state with an increasing cooling rate, indicating that faster cooling is beneficial to recovering the lost relaxation enthalpy due to structural relaxation and rejuvenating BMGs. The difference between DSC curves is approximately manifested in the temperature region of 420 K$\leqslant T\leqslant$500 K. Particularly, these effects are even strong: the intensity of the heat flow peak increases to 1.8 times upon decreasing the cooling rate from 20 to 1 K/min. Cooling from above T_g should fabricate a cooling rate-dependent structure, and its relaxation enthalpy is in direct proportion to the cooling rate. Moreover, the mechanical/physical properties of BMGs could be tailored or recovered by cooling from the above T_g. This outcome is the achievement of rejuvenation from the perspective of the glass formation process.

To quantify the rejuvenation induced by cooling, the rejuvenation enthalpy ΔH_{rej} is computed as $\Delta H_{rej}=\frac{1}{T_{heating}}\int_{T_s}^{T_e}W(T)\mathrm{d}T$, where $W(T)$ is the heat flow, $T_{heating}$ is the heating rate, and T_s and T_e correspond to the start and end temperatures of the region of difference between DSC curves, respectively. For our alloy, T_s=420 K and T_e=500 K.

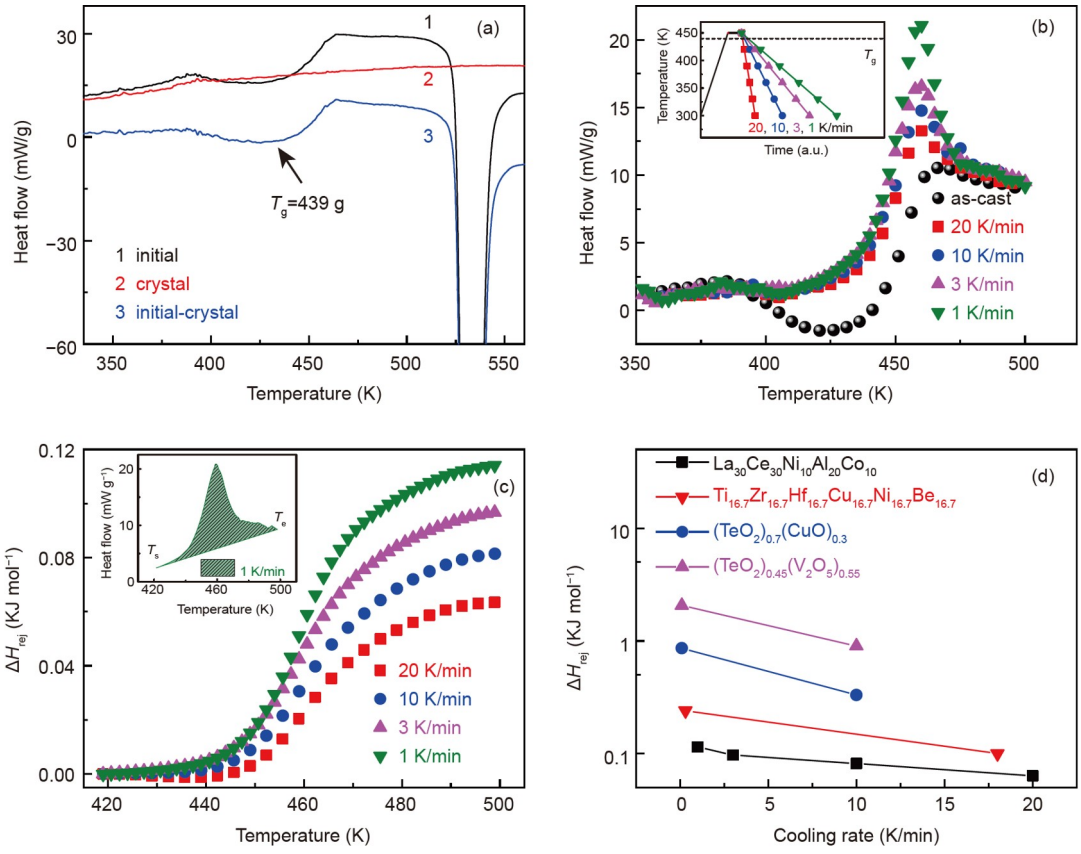

Figure 1 (Color online) (a) DSC traces carried out at 20 K/min of the $La_{30}Ce_{30}Ni_{10}Al_{20}Co_{10}$ BMG in the initial state (Run1) and after the full crystallization (Run2). The difference (Run1−Run2) gives the heat flow of the initial sample without any contribution to the crystalline state. (b) DSC traces after cooling from the SLR at various cooling rates. The inset shows the corresponding preceding cooling processes. (c) Evolution of the rejuvenation enthalpy on the temperature at various preceding cooling rates. The inset shows the start and end temperatures defined and used for the rejuvenation enthalpy calculations. (d) Correlation between the rejuvenation enthalpy and cooling rate of typical glasses (other results of typical glasses were obtained from the literature).

The inset of Figure 1(c) shows the calculation method with a dashed integration baseline. The evolution of ΔH_{rej} on the temperature at various preceding cooling rates is displayed in Figure 1(c). These curves trace almost identical paths, demonstrating that the structures are similar to one another. The more relaxation enthalpy lost during the preceding cooling process, the more enthalpy needed to be absorbed during heating to transition from glasses to supercooled liquids. The calculations result in ΔH_{rej}=0.12 kJ/mol for cooling rates of 20 K/min and 0.05 kJ/mol for 1 K/min, respectively. In addition, the typical glasses are classified based on the rejuvenation enthalpy by the DSC. Similar experimental results for $Ti_{16.7}Zr_{16.7}Hf_{16.7}Cu_{16.7}Ni_{16.7}$-$Be_{16.7}$ BMG, $(TeO_2)_{0.7}(Cu0)_{0.3}$ tellurite glass, and $(TeO_2)_{0.45}(V_2O_5)_{0.55}$ tellurite glass are exhibited in Figure 1(d) [22]. In particular, the rejuvenation enthalpies of BMGs are significantly lower than those of tellurite glasses. The parameter $S_r = -\Delta\left(\Delta H_{rej}\right) / \Delta\left(\Delta \dot{T}_{cooling}\right)$ was developed to level the sensitivity of the rejuvenation enthalpy of a glass to the change in the cooling rate. The values are computed as S_r=0.12, 0.054, 0.01, and 0.006 (kJ min)/(mol K) for $(TeO_2)_{0.45}(V_2O_5)_{0.55}$, $(TeO_2)_{0.7}(Cu0)_{0.3}$, $Ti_{16.7}Zr_{16.7}Hf_{16.7}$-$Cu_{16.7}Ni_{16.7}Be_{16.7}$, and $La_{30}Ce_{30}Ni_{10}Al_{20}Co_{10}$, respectively. Evidently, BMGs are less prone to be rejuvenated by cooling from the SLR compared with tellurite glasses because of their excellent thermal stability. This is also the reason why the rejuvenation of BMGs is extremely difficult but attractive.

Atomic mobility, a vital parameter to indicate the physical properties of BMGs, can be improved by typical thermal protocols and considerable plastic deformation [23,24]. In other words, physical aging and rejuvenation are closely correlated to multiple mechanical relaxation processes of BMGs. Here, the mechanical relaxation spectrum is performed to study the β- and α- relaxation processes originating from cooperative atomic rearrangements. Figure 2 shows the evolution of the normalized storage modulus E'/E_u and loss modulus E''/E_u on the temperature (E_u stands for the room-temperature storage modulus). The driving frequency is 2 Hz, and the heating rate is 2 K/min. The normalized loss modulus E''/E_u slightly decreases with the temperature when it is below 400 K, and a pronounced β relaxation peak

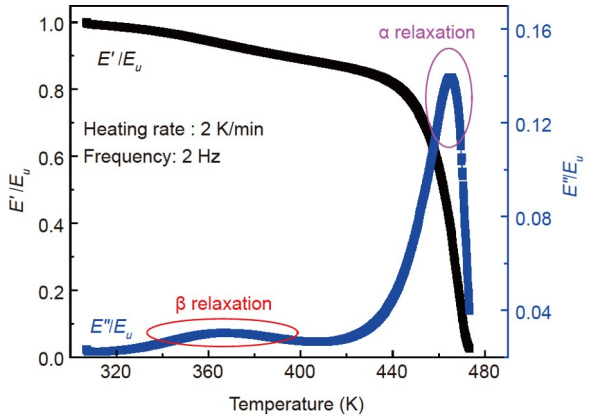

Figure 2 (Color online) Evolution of the normalized storage modulus E'/E_u and loss modulus E''/E_u on the temperature of the $La_{30}Ce_{30}Ni_{10}Al_{20}Co_{10}$ BMG.

emerges at around 367 K on the loss modulus curve. From 440 to 480 K, the normalized storage modulus E'/E_u drastically decreases while the maximum value of the normalized loss modulus E''/E_u corresponds to the αrelaxation. To further analyze the frequency dependence of the β- and α-relaxation processes, the isothermal relaxation spectra are scanned in a broadened frequency region from 315 to 465 K with an interval of 5 K. Two apparent temperature regions are shown in Figure 3(a) and (b): (1) At the low-temperature region, the storage modulus slightly decreases, while an apparent β relaxation dominates the low-temperature region of the E''/E_u curve. (2) At the high-temperature region, the storage modulus decreases, and a viscous flow can be activated by the applied mechanical stress in the SLR. Meanwhile, the loss modulus increases and reaches a maximum. Importantly, the β- and α-relaxation peaks shift to the higher-frequency region with increasing isothermal temperature, indicating that a high temperature accelerates the dynamic mechanical relaxation processes. Here, an Arrhenius equation in the form of $f = f_\beta \exp\left(-E_\beta / k_B T\right)$ was used to calculate the activation energy of the β relaxation E_β, where f is the driving frequency, k_B is the Boltzmann constant, and f_β is the characteristic frequency. Let us roughly assume that T_g is altered within a limited range by cooling. Thus, E_β can be regarded as a constant for our BMG. Compared with the as-cast sample (E_β=0.87 eV), E_β increases to 1.08 eV with a proceeding cooling rate of 10 K/min. Interestingly, this trend gets reversed with the decrease to 0.97 eV while increasing the cooling rate to 20 K/min. Generally, a high activation

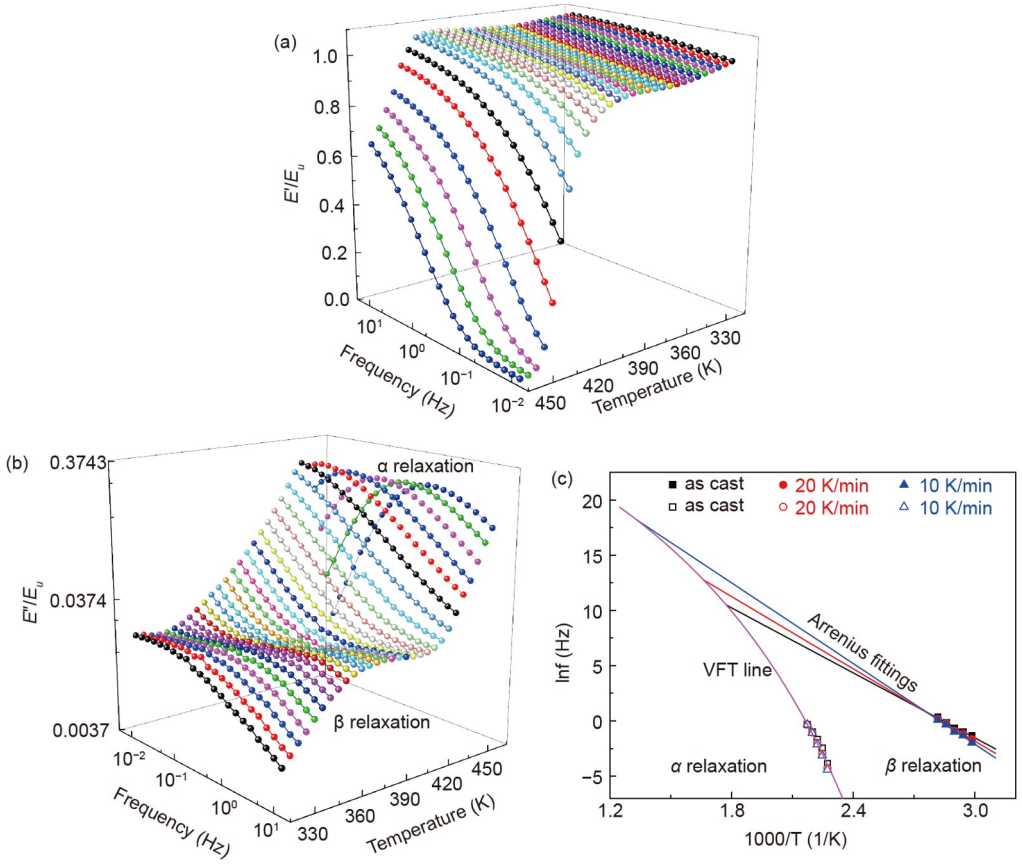

Figure 3 (Color online) Evolution of the normalized (a) storage modulus E'/E_u and (b) loss modulus E''/E_u on the driving frequency at different temperatures of the as-cast BMG. (c) Correlation between the peak temperature and driving frequency of the α relaxation and β relaxation in the $La_{30}Ce_{30}Ni_{10}Al_{20}Co_{10}$ BMG with different thermal histories. The frequency-dependent peak temperature of the α-relaxation process was fitted by the VFT function, whereas that of the β-relaxation process was fitted by the Arrhenius equation.

energy for the β relaxation is necessary to motivate local atomic rearrangements in a relaxed BMG. A fast cooling rate introduces a low β-relaxation activation energy, which is undoubtedly attributed to the improvement of the energetic state (or called rejuvenation). In brief, the resuscitation of the β-relaxation process demonstrates convincingly that many flow defects are created by a high cooling rate. Parallelly, the correlation between the frequency and α-relaxation peak temperature obeys the description of the Vogel-Fucher-Tammann (VFT) function in the form of $f=f_{\alpha}\exp(-B/T-T_0)$, where f_{α} is the characteristic frequency and B and T_0 are the fitting parameters [25]. The evolution of the frequency on the temperature of BMGs at different thermodynamic states almost traces the same VFT curve, although there is a slight difference among the peak frequency. The decoupling temperature T_c, where the β relaxation decouples from the α relaxation, effectively indicates the degree of the structural heterogeneity of BMGs. In the current work, T_c in the as-cast BMG is approximately 562 K. Interestingly, T_c increases with structural relaxation but decreases with rejuvenation. Previous works have reported that α relaxation is a globally rejuvenated process and can erase the structural relaxation induced by the thermal and mechanical history, which is characterized by the uniformity of atomic mobility [26]. The improvement of the mechanical relaxation processes of BMGs could be outlined in the concept of the potential energy landscape. The tailoring of the mechanical relaxation processes is induced by the density and distribution of sub-basins and the variation of coordinates in the configurational space. Because of such events, an apparent improvement in the quantity and distribution of flow defects can be achieved. The fast cooling from the SLR brings BMGs to a high-energy state and broadens the distribution of the sub-basins and then benefits the activation of the β relaxation.

We can portray the modulus/compliance master curve of glassy materials at the reference temperature in a broad frequency window via horizontal shifting based on the time-temperature superposition principle [27]. The moduli master curve of the $La_{30}Ce_{30}Ni_{10}Al_{20}Co_{10}$ BMG was obtained by shifting the isothermal results with the temperature shift factor $a_T=\tau(T)/\tau(T_{ref})$ and is shown in Figure 4(a), where $\tau(T)$ is the relaxation time at 450 K and $\tau(T_{ref})$ is that of the reference temperature T_{ref}. The master curve is primarily governed by the β relaxation at the high-frequency region, whereas the α-relaxation peak domains are at the low-frequency region. Figure 4(b) shows the composite master curves in the $La_{30}Ce_{30}Ni_{10}Al_{20}Co_{10}$ BMG for the loss modulus at different states. Evidently, structural relaxation suppresses the intensity of α- and β-relaxation processes, while faster cooling can comparatively counteract this tendency. Compared with the change in the β relaxation, the α-relaxation peak shifts toward a lower-frequency region. This large-scale rearrangement of atoms is unexpectedly tailored by the thermodynamic state of BMGs. Generally, the loss modulus of BMGs is directly correlated to their atomic mobility [28]. Importantly, the β relaxation of BMGs structurally origin from their heterogeneous microstructure, which is modeled as the random distribution of flow defects (loosely packed regions) and elastic matrix [16,29]. Hence, the deformation units in the loosely packed regions can be easily activated because of the low activation energy. Reasonably, the β-relaxation process, which is improved by faster cooling from the SLR, demonstrates the introduction of flow defects into the glassy structure.

The suggested physical model to describe the deformation mechanism of BMGs has generally fallen into two categories: (1) free volume (FV) [30], i.e., the order parameter

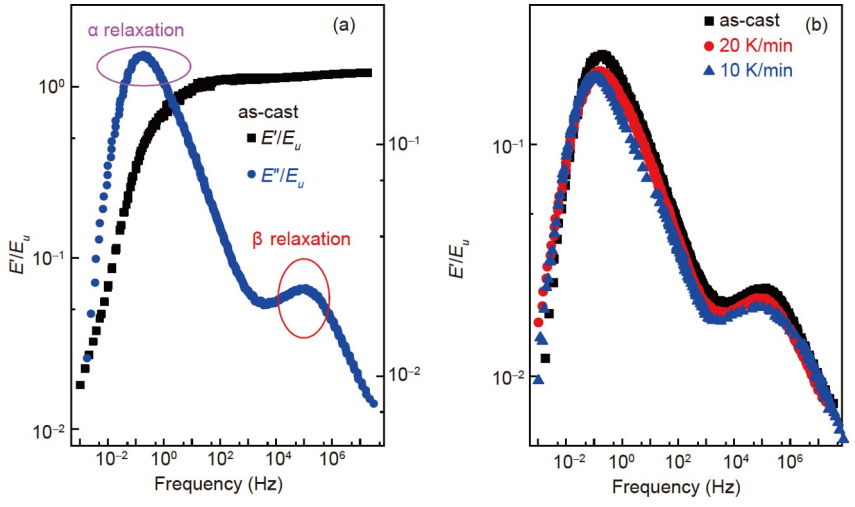

Figure 4 (Color online) (a) Master curves of the storage E'/E_u and loss modulus E''/E_u of the as-cast BMG within the frequency window at a reference temperature of 450 K. (b) Master curves in the $La_{30}Ce_{30}Ni_{10}Al_{20}Co_{10}$ BMG for the loss modulus E''/E_u in different states: as-cast and preceding cooling rates of 10 and 20 K/min, respectively.

for the macroscopic flow; (2) shear transformation zones (STZs) [31], i.e., the characteristic atomic clusters that undergo shear rearrangements. These essential mean-field theories are the mainstream explanations for the deformation of BMGs. However, the concept of using the concentration and orientation of FV/STZs as deformation indexes lacks a description of the correlation between different deformation units. The mechanical/physical properties are closely correlated to structural defects, although the definition of these defects is still unclear. Nowadays, the identification of liquid/solid-like regions is directly attributed to the apparent differences in the modulus, hardness, relaxation time, and activation energy, which agree with the fluctuation of the enthalpy and entropy on the nanoscale in the concept of quasi-point defect (QPD) theory [32]. In addition, the consideration of the interaction of the fluctuations of the enthalpy and entropy is highly effective in describing the mechanical relaxation processes and deformation mechanism. In other words, the concept of QPDs appears richer than that of STZs and FV. The temperature dependence of the loss factor tanδ of BMGs obeys the following equation [32]:

$$\ln(\tan\delta) = -\frac{U_\beta}{k_B T} - \chi \ln(2\pi f) + \lambda, \tag{1}$$

where U_β is the activation energy for the elementary units and correlates to the β-relaxation process, λ stands for a pre-parameter, and χ is the correlation factor that corresponds to the concentration and interplay between QPDs. When χ=0, the microstructure is highly ordered, and the movement of an elementary unit shows a dependence on others. When χ=1, the microstructure is highly disordered, and the movement of an elementary unit is totally individual. Here, we explore the correlation between the mechanical relaxation processes of BMGs and their microstructure to elucidate the physical mechanism of rejuvenation. The evolution of tanδ on the frequency at different temperatures of an as-cast BMG was fitted by eq. (1) regarding the activation process of QPDs (as shown in Figure 5(a)). The value of χ can be confirmed by the fitting lines. To facilitate comparison, Figure 5(b) shows the temperature-dependent correlation factor χ in various thermodynamic states. Clearly, the correlation of the correlation factor χ and temperature obeys a simple function, i.e.,

$$\begin{cases} \chi \propto a_1 T, T \leqslant T_g, \\ \chi \propto a_2 T, T \geqslant T_g, \end{cases} \tag{2}$$

where a_1 and a_2 are the rise rates with the temperature. Based on previous literature works, the value of χ generally lies in the range from 0.3 to 0.4 in various BMGs below the glass transition temperature T_g [33], where BMGs maintain the iso-configurational structural state. The correlation factor χ of the $La_{30}Ce_{30}Ni_{10}Al_{20}Co_{10}$ BMG slightly increases with the temperature below T_g. The evolution of the correlation factor χ is dependent on the thermodynamic state of BMGs. Structural relaxation induces a clear decrease of χ. With the increase in the preceding cooling rate, a rise of χ can be induced by rejuvenation. In addition, χ is correlated to the temperature-dependent QPD concentration. The calculated

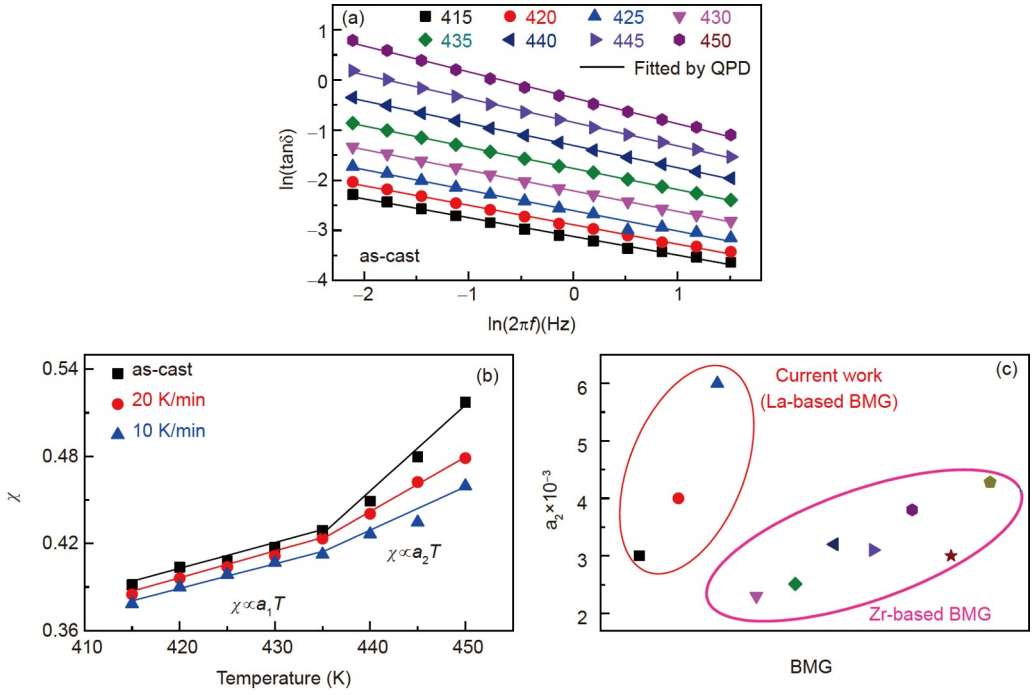

Figure 5 (Color online) (a) Evolution of the loss factor tanδ on the driving frequency at various temperatures of the as-cast BMG. The solid lines are fitted by the QPD model. (b) Evolution of the correlation factor χ with temperature in different states: as-cast and preceding cooling rates of 10 and 20 K/min, respectively. The solid lines are linear fittings. (c) Values of a_2 in typical glasses (fitting results of typical glasses were collected from the literature).

values of a_1 and a_2 are listed in Table 1. The rising rate a_1 when the temperature below T_g is independent of the thermodynamic state of BMGs indicates that structural relaxation/rejuvenation only alters the QPD concentration rather than their evolution in the iso-configurational state. As the temperature surpasses T_g, the atomic mobility of glassy materials gets significantly enhanced, so a drastic increase of χ can be observed. In addition, the rise rate a_2 increases with structural rejuvenation but decreases with structural relaxation. Hence, rejuvenation will enhance the degree of disorder of BMGs.

The comparison between the experimental results of a_2 in different glassy systems is summarized in Figure 5(c) (calculated results for various BMGs were collected from refs. [34,35]). The value of a_2 of the $La_{30}Ce_{30}Ni_{10}Al_{20}Co_{10}$ BMG is apparently higher than the reported Zr-based BMGs. Eq. (2) describes the degree of the non-Arrhenius relation of the α-relaxation time τ_α, which actually obeys the VFT relations. Meanwhile, parameter a_2 stands for the slope between $\ln(\tau_\alpha)$ and $1/T$, corresponding to the fragility of glassy systems [36]. Then, the value of a_2 becomes an index for the departure of the α-relaxation process from the Arrhenius description. It demonstrates that the fragility of the $La_{30}Ce_{30}Ni_{10}Al_{20}Co_{10}$ BMG is less than that of strong Zr-based BMGs.

Previous works mainly focus on the rapid cooling of a melting liquid to avoid crystallization, thereby preparing glasses [37]. From the aspect of classic thermodynamics, there is no discontinuity in the specific volume or enthalpy (as shown in the as-cast glass in Figure 6). In addition, T_g shows a strong dependence on the cooling rate, which is actually high to 10^3 K/s. A high cooling rate allows less time for configurational sampling, and then T_g increases with the cooling rate. BMGs prepared at high cooling rates possess more heterogeneous atomic structures and lower densities. Here, we show that cooling from the SLR is also one of the convenient methods to slightly improve the glassy properties, and the increases in the cooling rate have an equivalent role in rejuvenating BMGs. Therefore, a diagram of rejuvenation and structural relaxation via cooling from the SLR can be constructed, as shown in Figure 6.

4 Conclusions

In summary, our results validate the feasibility of the improvement of the mechanical properties of the $La_{30}Ce_{30}Ni_{10}Al_{20}Co_{10}$ BMG via cooling from the SLR at laboratory rates. The $La_{30}Ce_{30}Ni_{10}Al_{20}Co_{10}$ BMG shows the hardest rejuvenation propensity compared to other glasses. The increase in the cooling rate is beneficial to recovering the relaxation enthalpy lost upon structural relaxation, and so does the intensity of the β and α relaxations. In addition, the rise of the QPD concentration and creation rate demonstrates the improvement of dynamic heterogeneity.

Table 1 Values of a_1 and a_2 of the La-based BMG at different structural states

Structural state	$a_1\times10^{-3}$	$a_2\times10^{-3}$
As-cast	1.8	6
20 K/min	1.8	4
10 K/min	1.7	3

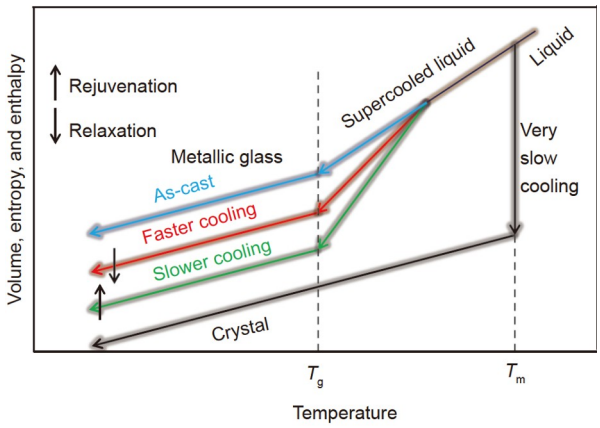

Figure 6 (Color online) Schematic illustration of rejuvenation and relaxation upon cooling from the SLR at the limitation of the negligible change of T_g. The properties, i.e., volume, entropy, and enthalpy, are used to evaluate the energetic state of BMGs. BMGs are actually produced by rapidly cooling the melting liquid to avoid crystallization. Here, the cooling from the SLR at a constant rate can fine-tune the properties of BMGs. A relatively high cooling rate can fabricate a rejuvenated BMG.

This work was supported by the National Natural Science Foundation of China (Grant Nos. 51971178 and 52271153), the Natural Science Basic Research Plan for Distinguished Young Scholars in Shaanxi Province (Grant No. 2021JC-12) and the Natural Science Foundation of Chongqing (Grant No. cstc2020jcyj-jqX0001). The investigation of LangTing ZHANG is sponsored by the Innovation Foundation for Doctor Dissertation of Northwestern Polytechnical University (Grant No. CX2021015). YunJiang WANG was financially supported by National Natural Science Foundation of China (Grant No. 12072344) and the Youth Innovation Promotion Association of the Chinese Academy of Sciences. Yong YANG acknowledges financial support from Research Grant Council (RGC) and the Hong Kong government through the General Research Fund (GRF) (Grant Nos. U11200719 and U11213118).

1 Qiao J C, Wang Q, Pelletier J M, et al. Structural heterogeneities and mechanical behavior of amorphous alloys. Prog Mater Sci, 2019, 104: 250–329
2 Johnson W. Thermodynamic and kinetic aspects of the crystal to glass transformation in metallic materials. Prog Mater Sci, 1986, 30: 81–134
3 Rao W, Chen Y, Dai L H. A constitutive model for metallic glasses based on two-temperature nonequilibrium thermodynamics. Int J Plast, 2022, 154: 103309
4 Kube S A, Sohn S, Ojeda-Mota R, et al. Compositional dependence of the fragility in metallic glass forming liquids. Nat Commun, 2022, 13: 3708
5 Zhang L T, Wang Y J, Pineda E, et al. Achieving structural rejuvenation in metallic glass by modulating β relaxation intensity via easy-to-operate mechanical cycling. Int J Plast, 2022, 157: 103402
6 Greer A L, Cheng Y Q, Ma E. Shear bands in metallic glasses. Mater Sci Eng-R-Rep, 2013, 74: 71–132

7 Lü Y J, Guo C C, Huang H S, et al. Quantized aging mode in metallic glass-forming liquids. Acta Mater, 2021, 211: 116873
8 Luckabauer M, Hayashi T, Kato H, et al. Decreasing activation energy of fast relaxation processes in a metallic glass during aging. Phys Rev B, 2019, 99: 140202
9 Pan J, Wang Y X, Guo Q, et al. Extreme rejuvenation and softening in a bulk metallic glass. Nat Commun, 2018, 9: 560
10 Ketov S V, Sun Y H, Nachum S, et al. Rejuvenation of metallic glasses by non-affine thermal strain. Nature, 2015, 524: 200–203
11 Sun Y, Concustell A, Greer A L. Thermomechanical processing of metallic glasses: Extending the range of the glassy state. Nat Rev Mater, 2016, 1: 16039
12 Ding G, Li C, Zaccone A, et al. Ultrafast extreme rejuvenation of metallic glasses by shock compression. Sci Adv, 2019, 5: eaaw6249
13 Pan J, Ivanov Y P, Zhou W H, et al. Strain-hardening and suppression of shear-banding in rejuvenated bulk metallic glass. Nature, 2020, 578: 559–562
14 Greer A L, Sun Y H. Stored energy in metallic glasses due to strains within the elastic limit. Philos Mag, 2016, 96: 1643–1663
15 Zhang L, Wang Y, Yang Y, et al. Aging and rejuvenation during high-temperature deformation in a metallic glass. Sci China-Phys Mech Astron, 2022, 65: 106111
16 Kosiba K, Şopu D, Scudino S, et al. Modulating heterogeneity and plasticity in bulk metallic glasses: Role of interfaces on shear banding. Int J Plast, 2019, 119: 156–170
17 Zhu F, Song S, Reddy K M, et al. Spatial heterogeneity as the structure feature for structure-property relationship of metallic glasses. Nat Commun, 2018, 9: 3965
18 Tsai P, Kranjc K, Flores K M. Hierarchical heterogeneity and an elastic microstructure observed in a metallic glass alloy. Acta Mater, 2017, 139: 11–20
19 Qiao J C, Zhang L T, Tong Y, et al. Mechancial properties of amorphous alloys: In the framework of the microstructure heterogeneity. Adv Mech, 2022, 52: 117–152
20 Küchemann S, Maaß R. Gamma relaxation in bulk metallic glasses. Scripta Mater, 2017, 137: 5–8
21 Jiang W, Zhang B. Strong beta relaxation in high entropy bulk metallic glasses. J Appl Phys, 2020, 117: 115104
22 Afonin G V, Zamyatin O A, Zamyatina E V, et al. Thermal rejuvenation of tellurite glasses by cooling from the supercooled liquid state at low rates. Scripta Mater, 2020, 186: 39–42
23 Stolpe M, Kruzic J J, Busch R. Evolution of shear bands, free volume and hardness during cold rolling of a Zr-based bulk metallic glass. Acta Mater, 2014, 64: 231–240
24 Zhang L T, Duan Y J, Pineda E, et al. Effect of physical aging and cyclic loading on power-law creep of high-entropy metallic glass. J Mater Sci Technol, 2022, 115: 1–9
25 Böhmer R, Ngai K L, Angell C A, et al. Nonexponential relaxations in strong and fragile glass formers. J Chem Phys, 1993, 99: 4201–4209
26 Wang W H. Dynamic relaxations and relaxation-property relationships in metallic glasses. Prog Mater Sci, 2019, 106: 100561
27 Zhang L T, Duan Y J, Crespo D, et al. Dynamic mechanical relaxation and thermal creep of high-entropy $La_{30}Ce_{30}Ni_{10}Al_{20}Co_{10}$ bulk metallic glass. Sci China-Phys Mech Astron, 2021, 64: 296111
28 Wang B, Wang L J, Shang B S, et al. Revealing the ultra-low-temperature relaxation peak in a model metallic glass. Acta Mater, 2020, 195: 611–620
29 Dmowski W, Iwashita T, Chuang C P, et al. Elastic heterogeneity in metallic glasses. Phys Rev Lett, 2010, 105: 205502
30 Spaepen F. Homogeneous flow of metallic glasses: A free volume perspective. Scripta Mater, 2006, 54: 363–367
31 Argon A S. Plastic deformation in metallic glasses. Acta Metall, 1979, 27: 47–58
32 Perez J. Quasi-punctual defects in vitreous solids and liquid-glass transition. Solid State Ion, 1990, 39: 69–79
33 Hao Q, Lyu G J, Pineda E, et al. A hierarchically correlated flow defect model for metallic glass: Universal understanding of stress relaxation and creep. Int J Plast, 2022, 154: 103288
34 Qiao J C, Cong J, Wang Q, et al. Effects of iron addition on the dynamic mechanical relaxation of $Zr_{55}Cu_{30}Ni_5Al_{10}$ bulk metallic glasses. J Alloys Compd, 2018, 749: 262–267
35 Wang C H, Hu Y J, Qiao J C, et al. Mechanical relaxation behavior of $Zr_{64.13}Cu_{15.75}Ni_{10.12}Al_{10}$ bulk metallic glass. Mater Sci Eng-A, 2018, 738: 57–62
36 Angell C A, Ngai K L, McKenna G B, et al. Relaxation in glass-forming liquids and amorphous solids. J Appl Phys, 2000, 88: 3113–3157
37 Wada T, Inoue A. Formation of porous Pd-based bulk glassy alloys by a high hydrogen pressure melting-water quenching method and their mechanical properties. Mater Trans, 2004, 45: 2761–2765